Redox Biology 72 (2024) 103135

Contents lists available at ScienceDirect

Redox Biology

journal homepage: www.elsevier.com/locate/redox

Melanoma-associated melanocortin 1 receptor variants confer redox signaling-dependent protection against oxidative DNA damage

María Castejón-Griñán **, Sonia Cerdido, José Sánchez-Beltrán, Ana Lambertos, Marta Abrisqueta, Cecilia Herraiz, Celia Jiménez-Cervantes, José Carlos García-Borrón *

Department of Biochemistry, Molecular Biology and Immunology, School of Medicine, University of Murcia and Biomedical Research Institute of Murcia (Instituto Murciano de Investigación Biosanitaria, IMIB), El Palmar, Murcia, Spain

ARTICLE INFO

Keywords:
Melanocortin 1 receptor (MC1R)
Oxidative DNA damage
Melanoma
Reactive oxygen species (ROS)
Base excision repair (BER)

ABSTRACT

Cutaneous melanoma, a lethal skin cancer, arises from malignant transformation of melanocytes. Solar ultraviolet radiation (UVR) is a major environmental risk factor for melanoma since its interaction with the skin generates DNA damage, either directly or indirectly via oxidative stress. Pheomelanin pigments exacerbate oxidative stress in melanocytes by UVR-dependent and independent mechanisms. Thus, oxidative stress is considered to contribute to melanomagenesis, particularly in people with pheomelanic pigmentation. The melanocortin 1 receptor gene (*MC1R*) is a major melanoma susceptibility gene. Frequent *MC1R* variants (varMC1R) associated with fair skin and red or yellow hair color display hypomorphic signaling to the cAMP pathway and are associated with higher melanoma risk. This association is thought to be due to production of photosensitizing pheomelanins as well as deficient induction of DNA damage repair downstream of varMC1R. However, the data on modulation of oxidative DNA damage repair by MC1R remain scarce. We recently demonstrated that varMC1R accelerates clearance of reactive oxygen species (ROS)-induced DNA strand breaks in an AKT-dependent manner. Here we show that varMC1R also protects against ROS-dependent formation of 8-oxodG, the most frequent oxidative DNA lesion. Since the base excision repair (BER) pathway mediates clearance of these DNA lesions, we analyzed induction of BER enzymes in human melanoma cells of *varMC1R* genotype. Agonist-mediated activation of both wildtype (wtMC1R) and varMC1R significantly induced OGG and APE-1/Ref1, the rate-limiting BER enzymes responsible for repair of 8-oxodG. Moreover, we found that NADPH oxidase (NOX)-dependent generation of ROS was responsible for AKT activation and oxidative DNA damage repair downstream of varMC1R. These observations provide a better understanding of the functional properties of melanoma-associated *MC1R* alleles and may be useful for the rational development of strategies to correct defective varMC1R responses for efficient photoprotection and melanoma prevention in fair-skinned individuals.

1. Introduction

Cutaneous melanoma is a lethal skin cancer that arises from the malignant transformation of melanocytes. The interaction of ultraviolet radiation (UVR) with the skin generates DNA damage, thus making solar UVR a major risk factor for melanoma and non-melanoma skin cancer [1,2]. Direct absorption of energetic UVB photons by DNA triggers the formation of pyrimidine dimers, mainly cyclobutane pyrimidine dimers (CPDs) [3] and pyrimidine (6-4) pyrimidone photoproducts (6-4 PPs) [4,5]. CPDs, responsible for a UVR mutation signature (C → T transitions), are associated with 90% of non-melanoma skin cancers and 60% of melanomas [2,6,7]. The less energetic UVA component of solar UVR can also damage DNA indirectly via oxidative stress by production of reactive oxygen species (ROS) causing oxidative lesions, mainly 8-oxo-7,8-dihydroguanine (8-oxodG) and DNA strand breaks (SBs) [8]. Importantly, while darker eumelanins formed within melanocytes are photoprotective pigments, lighter yellow-reddish pheomelanin pigments can act as photosensitizers boosting the generation of ROS in UVR-exposed skin [1]. However, although the presence of pheomelanin leads to

* Corresponding author.
** Corresponding author.
E-mail addresses: maria.castejon1@um.es (M. Castejón-Griñán), sonia.cerdidoo@um.es (S. Cerdido), jose.sanchezb@um.es (J. Sánchez-Beltrán), ana.lambertos@um.es (A. Lambertos), marta.ag@um.es (M. Abrisqueta), ceciliahs@um.es (C. Herraiz), celiajim@um.es (C. Jiménez-Cervantes), gborron@um.es (J.C. García-Borrón).

https://doi.org/10.1016/j.redox.2024.103135
Received 12 February 2024; Received in revised form 12 March 2024; Accepted 25 March 2024
Available online 26 March 2024

Abbreviations

APE-1/Ref1	apurinic/apyrimidinic endonuclease 1/redox effector-1
BER	base excision repair
CPD	cyclobutane pyrimidine dimer
DCF	2′,7′-dichlorofluorescein
DDA	2′5′-dideoxyadenosine
DPI	diphenylepodium
GPCR	G protein-coupled receptor
H_2DCFDA	2′7′-dichlorodihydrofluorescein diacetate
HMC	human melanoma cell
Luperox®	*tert*-Butyl hydroperoxide
MC1R	melanocortin 1 receptor
αMSH	α melanocyte-stimulating hormone
NDP-MSH	[Nle4, D-Phe7] αMSH
NER	nucleotide excision repair
NOX	NADPH oxidase
OGG	8-oxoguanine DNA glycosylase/AP lyase
8-oxodG	8-oxo-7,8-dihydroguanine
6-4 PP	pyrimidine (6-4) pyrimidone photoproduct
RHC	Red Hair Color
ROS	reactive oxygen species
SB	strand break
UVR	ultraviolet radiation
varMC1R	variant MC1R
wtMC1R	wildtype MC1R

chronic oxidative stress and is associated with a higher burden of oxidative damage in melanocytes than in other types of skin cells, the contribution of these lesions to melanomagenesis remains uncertain [9].

The melanocortin 1 receptor (MC1R), a G-protein coupled receptor (GPCR) expressed in melanocytes [10], plays a central role in regulating the cutaneous responses to UVR [11] and is considered a central regulator of protection against oxidative stress in melanocytes [12]. In UVR-exposed skin, keratinocytes stimulate the production of melanocortin peptides, notably α melanocyte-stimulating hormone (αMSH), that act in a paracrine manner to stimulate, via cAMP signaling, the switch from basal synthesis of photosensitizing pheomelanins to eumelanogenesis within melanocytes [1,2]. Therefore, MC1R signaling determines the amount and type of pigment produced by melanocytes, since low or absent MC1R activity is associated with pheomelanogenesis whereas strong signaling leads to the production of brown-black eumelanins [11].

The human *MC1R* gene (MIM# 155555, Ensembl ID ENSG00000258839) is unusually polymorphic, with around 200 coding region allelic variants described to date [11,13]. Due to their hypomorphic signaling to the cAMP pathway [14,15], many *MC1R* natural variants fail to activate eumelanin synthesis properly, resulting in higher contents of pheomelanin. These variants are strongly associated with the "Red Hair Color" (RHC) phenotype, characterized by fair skin, red hair color, freckles, propensity to sunburn, inability to tan and increased melanoma and non-melanoma skin cancer risk [16–18]. According to their penetrance for the RHC phenotype, *MC1R* variants have been categorized into strong "R" or weaker "r" alleles [19]. The *MC1R* genotype also influences the mutational load in melanoma, since carrying at least one *RHC* allele increases the burden of the UVR mutational signature as well as non-UVR base pair substitutions [20,21].

Since MC1R activity promotes the pheo-to-eumelanogenesis switch, it is widely accepted that a pigmentation-dependent effect most likely accounts, at least partially, for the increased melanoma risk in carriers of RHC variants [22]. However, variant MC1R (varMC1R) confers increased melanoma risk even in dark-skinned populations, thus suggesting the relevance of non-pigmentary MC1R actions [23–27]. Indeed, MC1R orchestrates a complex series of events to induce antioxidant defenses [28,29] and DNA repair responses in UVR-exposed melanocytes [13,30]. Since most of these pigment-independent effects are thought to rely on the cAMP signaling pathway, it is generally assumed that reduced cAMP signaling downstream of hypomorphic varMC1R would compromise the induction of DNA repair [11,31–33] and antioxidant activities [28,29,34], thus increasing mutation rates and melanoma risk. However, several major R-type RHC variants have been shown to display functional coupling to the ERK pathway comparable to the wildtype receptor (wtMC1R) and are able to stimulate AKT [13,14,35,36]. Therefore, they behave as biased signaling forms rather than as classical loss-of-function variants. Moreover, previous work from our group showed that in human melanoma cells (HMCs) carrying R-type varMC1R, an MC1R agonist activated AKT signaling to induce clearance of DNA strand breaks (SBs) formed upon an oxidative challenge [36]. Yet, neither the signaling pathway accounting for AKT activation downstream of varMC1R nor the DNA repair pathways responsible for clearance of oxidative lesions downstream of either wt or varMC1R were elucidated.

Using a combination of genetic and pharmacologic approaches, here we show that agonist-mediated activation of both wt and varMC1R promoted induction of the base excision repair (BER) enzymes responsible for repair of 8-oxodG. We also show that downstream of varMC1R, NADPH oxidase (NOX)-dependent generation of ROS led to AKT activation to promote induction of BER enzymes and repair of DNA oxidative damage.

2. Materials and methods

2.1. Reagents

Igepal CA-630, BSA, EDTA, PMSF, iodoacetamide, bicinchoninic acid, *tert*-Butyl hydroperoxide solution (Luperox® TBH70X), 2′5′-Dideoxyadenosine (DDA), the AKT activator SC79 and the NOX inhibitor Diphenylepodium (DPI) were from Sigma (St. Louis, MO). The phosphatase inhibitor mix and the synthetic αMSH analogue [Nle4, D-Phe7] αMSH (NDP-MSH) were from Calbiochem (Darmstadt, Germany). The AKT1/2/3 inhibitor MK-2206, the PI3K inhibitor LY294002 and the NOX1/4 inhibitor GKT137831 were from Apexbio Technology LLC (Houston, USA). Reagents used for SDS-PAGE and Western blot were from Bio-Rad (Richmond, CA, USA). Other reagents were from Merck (Darmstadt, Germany).

2.2. Cell culture

HBL (LOCE-MM1) were kindly provided by Prof. G. Ghanem, LOCE-Institut J. Bordet, Université Libre de Bruxelles, Belgium. All HMCs were grown in DMEM with 10% fetal bovine serum (FBS), 100 U/ml penicillin and 100 μg/ml streptomycin sulfate. Serum was removed 1 day before and for the duration of each experiment. Cell culture reagents and trypsin/EDTA were from Gibco (Gaithersburg, MD). All cells were incubated at 5% CO_2 and 37 °C.

2.3. ROS measurements

ROS levels were determined by two fluorescent methods, depending on ROS subcellular localization. Production of intracellular ROS was assessed with the cell-permeant probe 2′7′-dichlorodihydrofluorescein diacetate (H_2DCFDA) (Molecular Probes, Invitrogen). DCFDA is de-esterified by intracellular esterases and turns to highly fluorescent 2′,7′-dichlorofluorescein (DCF) upon oxidation by ROS. Cells were grown in DMEM without phenol red in a 96-well white microplate,

serum-deprived for at least 3 h and treated as required. Then cells were washed with PBS and incubated with 10 μM DCFDA dye in Hank's Balanced Salt Solution for 45 min at 37 °C and 5 % CO_2, washed again and treated with Luperox or NDP-MSH, as required. Cells were washed 3 times with PBS and fluorescence was measured at 492 nm excitation and 517 nm emission in a microplate reader. Cells incubated with Hank's without DCFDA were used as negative control. Background fluorescent values were subtracted from signal fluorescent values.

To assess extracellular ROS levels, we used Amplex UltraRed (Molecular Probes, Invitrogen). This dye is an impermeant reagent that can be oxidized in the presence of a peroxidase to produce resorufin, a fluorescent reaction product. Cells were grown as above, treated as required, and washed with PBS. Then a working-solution containing 50 μmol/L Amplex® Red reagent and 0.1 U/ml horseradish peroxidase in Krebs-Ringer phosphate (145 mmol/L NaCl, 5.7 mmol/L sodium phosphate, 4.86 mmol/L KCl, 0.54 mmol/L $CaCl_2$, 1.22 mmol/L $MgSO_4$, 5.5 mmol/L glucose, pH 7.35) was added into each well. Fluorescence was measured at 530 nm excitation and 590 nm emission at multiple time-points and corrected for background with appropriate blanks.

In both assays, fluorescence intensity signals were normalized for cell density with crystal violet. To this end, 20 μl of 0.5 % crystal violet in acetic acid was added into each well containing 100 μl of the corresponding buffer, and the microplate was incubated for 10 min at room temperature in the dark. Cells were washed with water, allowed to air-dry, and solubilized with methanol. Absorbance was measured at 562 nm on a microtiter plate reader. Fluorescent values at 517 nm or 590 nm (ROS signal) were normalized to absorbances at 562 nm (crystal violet). Unless otherwise specified, at least 3 independent experiments were performed, with at least triplicate wells for each time-point.

2.4. cAMP measurements

cAMP intracellular levels were measured by means of a commercial enzyme immunoassay (R&D Systems), as previously described [36]. Briefly, cells grown in 12-well plates were serum-deprived for at least 3 h and stimulated for 30 min with 100 nmol/L NDP–MSH. The medium was removed, and the cells were quickly washed with 800 μl ice-cold PBS, lysed with 200 μl/well 0.1 N HCl, and scrapped. The mix was freeze-dried, washed with 100 μl H_2O and freeze-dried again. Enzyme immunoassay was then performed as per instructions from the manufacturer. Parallel dishes were used for protein determination with bicinchoninic acid.

2.5. Immunoblotting

Cells were lysed in solubilization buffer (50 mmol/L Tris-HCl pH 7.5, 1% Igepal, 1 mmol/L EDTA, 0.1 mmol/L PMSF, 10 mmol/L iodoacetamide and 1% phosphatase inhibitor mix) at 4 °C for 1 h. Protein concentration in cell lysates was determined by the bicinchoninic acid assay according to supplier's instructions. Volumes containing 10 μg protein were mixed (2:1 ratio) with electrophoresis sample buffer (60 mmol/L Tris–HCl, pH 6.8, 5% glycerol, 3% SDS, 2.5% bromophenol blue and 1.0 mol/L β-mercaptoethanol). Western blotting was carried out as described previously [37]. Antibodies used are summarized in Supplementary Table 1. Band intensities were estimated with ImageJ software (National Institutes of Health, Bethesda, MA, USA), and were normalized to loading controls.

2.6. Immunofluorescence, confocal microscopy, and image quantification

The antibodies used for immunochemical detection of 8-oxodG and apurinic/apyrimidinic endonuclease 1/redox effector-1 (APE-1/Ref1) are specified in Supplementary Table 2. Cells were seeded in 24-well plates containing sterile coverslips, grown to 60 % confluency and treated as required. For 8-oxodG staining, we followed the protocol described in Ref. [36]. DAPI was used for nuclear staining. For APE-1/Ref1 staining, cells were fixed with 4% p-formaldehyde, permeabilized with 0.5% Triton-X 100 (v/v), blocked with 5% BSA in PBS (1 h, room temperature) and labeled with an anti-APE-1 monoclonal antibody (Santa Cruz Biotechnology, Cambridge, UK), followed by an Alexa 488-conjugated secondary antibody. After immunostaining, samples were mounted with a medium from Dako (Glostrup, Denmark) and examined with a Leica laser scanning confocal microscope with 63x objective lens and software (Leica Microsystems GmbH, Wetzlar, Germany). Laser power, gain and offset were established for each fluorophore to minimize background, sample saturation and photobleaching. For 8-oxodG and APE-1/Ref1 immunostainings, at least ten randomly selected images of the coverslip were acquired (corresponding to at least 300 cells). To select z position of each image, maximum intensity of nuclei signal (DAPI channel) was used. Each fluorophore emission was collected separately, and both images were acquired exactly in the same position. All cells in the images were quantified. Mean signal intensities were analyzed and quantified with a semi-automatic macro generated in ImageJ software. Briefly, cell nuclei areas were selected according to their emitted fluorescence corresponding to DAPI staining with the "analyze particles" plugin, and the nuclei perimeter was delimited. Nuclear APE-1/Ref-1 and 8-oxodG signals within this region of interest were quantified calculating the pixel intensity in single cell nuclei relative to the nucleus area. All values were normalized to the average signal intensity of the control condition.

2.7. Generation of CRISPR/Cas9-based MC1R-KO cells and reconstitution with defined MC1R variants

Cells expressing wtMC1R or the R-type R151C variant on an isogenic background were obtained by a previously published procedure [38]. Briefly, a sgRNA consisting of the 20-nt guide sequence 5′-catcgcctactacgaccacg-3' (spanning nucleotides 536 to 556 in the open reading frame of the *MC1R* gene, corresponding to part of the fourth transmembrane fragment of the MC1R protein) was designed, whose efficiency and potential off-targets were determined with the Breaking-Cas tool (http://bioinfogp.cnb.csic.es/tools/breakincas) [39]. sgRNA oligonucleotides (Dharmacon, Lafayette, CO) were cloned into the pSpCas9(BB)-2A-Puro Cas9 Nuclease Expression plasmid, v2.0 (Addgene plasmid ID: 62988). Next, HBL cells were transfected with 1.0 μg of the resulting plasmid and 2.0 μg of Lipofectamine 2000. For negative control cells, we transfected the original vector with no insert. Puromycin-resistant clonal cells were selected with 1 μg/ml puromycin. Confirmation and selection of MC1R-KO clones was performed by sequencing and by lack of detectable cAMP production following NDP-MSH stimulation.

Stable transfectants expressing the Flag-tagged wildtype or R151C MC1R forms on the MC1R-null isogenic background provided by a clone of MC1R-KO cells were obtained as described elsewhere, using the corresponding cDNAs cloned into the pcDNA3 expression vector [37]. Suitable clones of MC1R-expressing cells were ascertained by Western blotting with the anti-Flag M2 monoclonal antibody from Merck and were cultured in the continuous presence of 800 μg/ml G418 sulfate.

2.8. siRNA-mediated knockdown of AKT and NOX1 expression

All the oligonucleotides employed were from Dharmacon. For knockdown of AKT expression, pilot experiments were performed by transfecting A375 and/or SKMEL28 for 24 h with control non-targeting siRNA, or individual siRNA directed against either AKT-1, AKT-2 or AKT-3, at a final concentration of 30 nmol/L (catalog number M-003000-03-0005, M-003001-02-0005, M-003002-02-0005, respectively). These siRNA targeting specific AKT isoenzymes all achieved significant but partial reduction of AKT expression. Accordingly, to increase the efficiency of knockdown, we used routinely a stoichiometric mixture of siRNA oligonucleotides targeting AKT-1, AKT-2 and AKT-3 at a final concentration of 20 nmol/L each. For NOX1 knockdown, a single

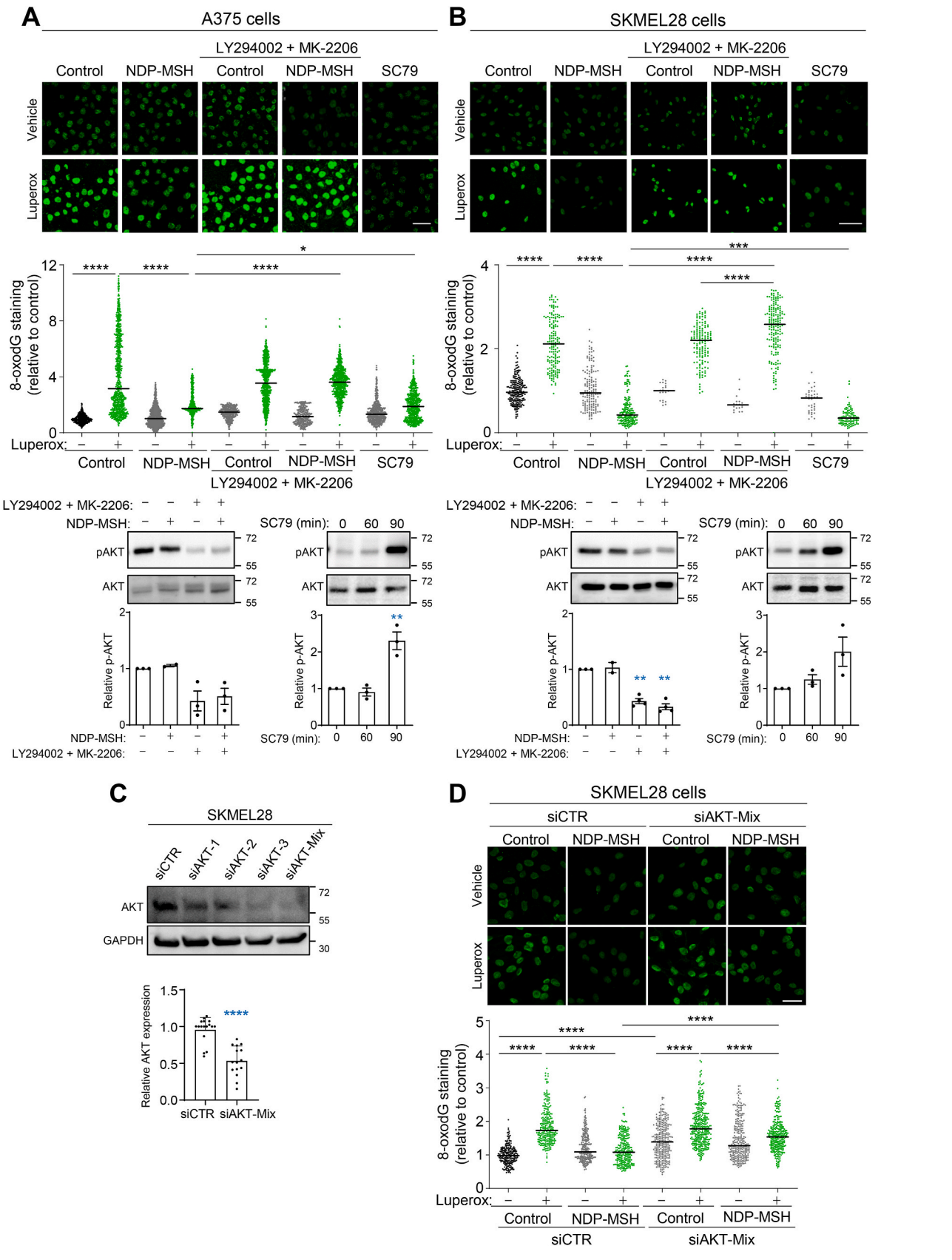

(caption on next page)

Fig. 1. Involvement of AKT in varMC1R-dependent protection against oxidative DNA damage. A375 (**A**) and SKMEL28 (**B**) melanoma cells were pretreated for 1 h with LY294002 (20 μmol/L) and MK-2206 (5 μmol/L) to block AKT activation, then stimulated with NDP-MSH (100 nmol/L, 36 h) prior to treatment with Luperox (0.15 mmol/L, 20 min). Cells were also treated with SC79 (10 μg/ml, 36 h), an activator of AKT, before the Luperox challenge. After the oxidative challenge, the cells were immunostained for 8-oxodG, and the intensity of the signal was quantified for at least 300 cells on each replicate. Representative confocal images are shown (bar size: 50 μm). The bar graph below the confocal images presents the quantitative analysis of nuclear 8-oxodG fluorescence intensity in each condition, normalized to the average signal of the untreated controls (n = 3 independent experiments). Representative inmunoblots showing phospho-AKT levels after treatment with NDP-MSH in the presence or absence of AKT inhibitors (left) and SC79 (right) are shown as a control for efficient inhibition by LY294002/MK2206 or activation by SC79. Quantification of the intensity of pAKT signal relative to the control is shown below. Total AKT1/2/3 was used as loading control (n = 3, error bars are mean ± SEM). **(C) siRNA-mediated silencing of AKT expression in SKMEL28 cells.** Cells were treated with control non-targeting siRNA (siCTR) or with siRNAs targeting specific AKT isoenzymes (siAKT-1, -2 or -3), or their stoichiometric mixture (siAKT-Mix). The levels of total AKT were compared by Western blot using a panAKT antibody. A representative blot is shown, with the quantification below (n > 15). **(D) Inhibition of varMC1R-dependent protection against oxidative damage upon repression of AKT.** SKMEL 28 cells were pretreated with control siRNA or with a stoichiometric mix of siRNAs targeting the individual AKT isoenzymes before stimulation with NDP-MSH (100 nmol/L, 24h). Then, cells were challenged with Luperox (0.15 mmol/L, 20 min), fixed and immunostained for 8-oxodG. Images were taken and quantified as in panels A and B (n = 3 independent experiments).

targeting siRNA was used (catalog number MQ-010193-01-0002) at a final concentration of 50 nmol/L. In all cases, OptiMEM and 5 μl/well DharmaFECT 4 transfection reagent was used. After transfection, cells were kept for 48 h in DMEM-GlutaMAX before analysis.

2.9. Statistical analysis

Statistical analysis was performed using GraphPad Prism (GraphPad Software, San Diego California, USA), comparing two groups unless otherwise specified. Normality tests were performed and, for experimental data with a normal distribution, unpaired two-tailed Student's t-tests were employed, with or without Welch's correction, depending on variance comparison. For non-normal distributions, the Mann-Whitney test was employed. Data were presented as scatter dot plots with median (for confocal images) or with mean ± standard error mean (SEM) for Western blots, cAMP and ROS measurements. p values lower than 0.05 were considered statistically significant (* indicates $p < 0.05$, ** $p < 0.01$, *** $p < 0.001$ and **** $p < 0.0001$; ns stands for not significant). Experiments were performed with at least three biological replicates.

3. Results

3.1. AKT activation is required for varMC1R-induced repair of 8-oxodG

The most prevalent oxidative lesion in DNA is the formation of 8-oxodG, followed by SBs and other oxidized pyrimidines [9,40]. Our previous work on repair of oxidative damage in HMCs showed the involvement of an MC1R-AKT pathway in the clearance of DNA SBs in cells of *varMC1R* genotype [36], but the role of AKT in the repair of oxidized DNA bases was not formally shown. Therefore, we aimed at confirming the dependence on AKT of 8-oxodG clearance downstream of varMC1R. We used two different HMC lines harboring the V600E BRAF mutation, A375 and SKMEL28. A375 cells are homozygous for the R151C *varMC1R* and SKMEL28 cells are heterozygous for two loss-of-function *MC1R* alleles (I155T and S83P), resulting in complete absence of cAMP signaling [36]. Cells were challenged with *tert*-butyl hydroperoxide (Luperox), a stable peroxide, either with or without pretreatment with the αMSH analogue NDP-MSH, and 8-oxodG was detected by immunocytochemistry. As expected, Luperox treatment increased 8-oxodG levels, whereas pretreatment with NDP-MSH significantly diminished this increase (Fig. 1A and B). To confirm the involvement of AKT in this varMC1R-dependent protective effect, cells were preincubated with the inhibitors of the PI3K/AKT pathway LY94002 and MK-2206 targeting PI3K and AKT respectively. PI3K/AKT inhibition abolished the reduction of 8-oxodG levels afforded by activation of varMC1R in both cell lines (Fig. 1A and B). The protective effect of AKT activation was verified by performing the oxidative challenge in cells pretreated with SC79, an agonist which binds to AKT to induce phosphorylation by upstream activatory kinases [41]. This drug decreased 8-oxodG levels in Luperox-treated A375 and SKMEL28 cells. Therefore, activation of the PI3K/AKT pathway downstream of varMC1R seemed sufficient to decrease the 8-oxodG burden in HMCs undergoing oxidative stress and was required for NDP-MSH-induced clearance of 8-oxodG lesions.

Next, we aimed at confirming the proposed role of AKT by testing the effects of its repression with siRNA on the genoprotective action of varMC1R. There are three closely related AKT isoforms, AKT1, AKT2 and AKT3, encoded for by different genes [55]. The three isoforms are widely expressed, with low or absent tissue specificity (proteinatlas.org). In agreement with these data, different siRNAs specifically targeting each AKT isoenzyme achieved a partial reduction of the total AKT signal detected with a pan-AKT antibody (Fig. 1C). Accordingly, we used a stoichiometric mix of oligonucleotides (20 nmol/L each) targeting AKT1, 2 and 3. This mix decreased AKT expression to residual levels around 50% (Fig. 1D), without a significant effect on cell viability during the time course of the experiments (data not shown). SKMEL28 cells treated with control (siCTR) or AKT-directed (siAKT) siRNA were challenged with Luperox and analyzed for 8-oxodG. As expected, the peroxide increased 8-oxodG in siCTR-treated cells, and this increase was efficiently blocked by pretreatment with NDP-MSH (Fig. 1D). Notably, repression of AKT caused a significant increase in the 8-oxodG burden of SKMEL28 cells in the absence of the oxidative challenge, suggesting that AKT might be required to cope with endogenous oxidative DNA damage. Moreover, downregulation of AKT significantly impaired the protective response to NDP-MSH. Indeed, the oxidative challenge increased 8-oxodG levels even after pretreatment with the MC1R agonist, and the resulting levels of oxidized base were higher after AKT downregulation than in siCTR-treated cells challenged in the same conditions (Fig. 1D).

These experiments aiming at demonstrating varMC1R-induced, AKT-dependent reduction of 8-oxodG were performed using cell lines of different genetic background. Moreover, in these cells, an aberrant expression of melanocortin receptor subtypes different from MC1R that may contribute to the protective responses triggered by NDP-MSH could not be excluded. Therefore, we sought to confirm protection against oxidative damage downstream of either varMC1R or wtMC1R in a different cellular setting and in cells of identical genetic background. To this end, we knocked out the *MC1R* gene in HBL HMCs using a CRISPR-Cas9 protocol. Complete MC1R ablation and lack of any other NDP-MSH-responsive melanocortin receptor in the resulting MC1R-KO cells was verified by absence of activation of cAMP synthesis by NDP-MSH [38] (Supplementary Fig. 1A). Then, MC1R-KO cells were transfected to express stably Flag epitope-tagged wt or variant (R151C) MC1R, and clones of the resulting cells expressing comparable levels of the receptor protein were selected (Supplementary Fig. 1B). Finally, MC1R-KO, MC1R-WT and MC1R-R151C cells were challenged with Luperox, either with or without pretreatment with NDP-MSH, and analyzed for 8-oxodG. As expected, NDP-MSH failed to afford significant protection against 8-oxodG accumulation in Luperox-challenged MC1R-KO cells (Supplementary Fig. 1C, left panel). In cells expressing wtMC1R, pretreatment with NDP-MSH prevented the accumulation of DNA oxidative damage after the Luperox challenge (Supplementary Fig. 1C, middle panel). Cells expressing varMC1R (MC1R-R151C cells) were also

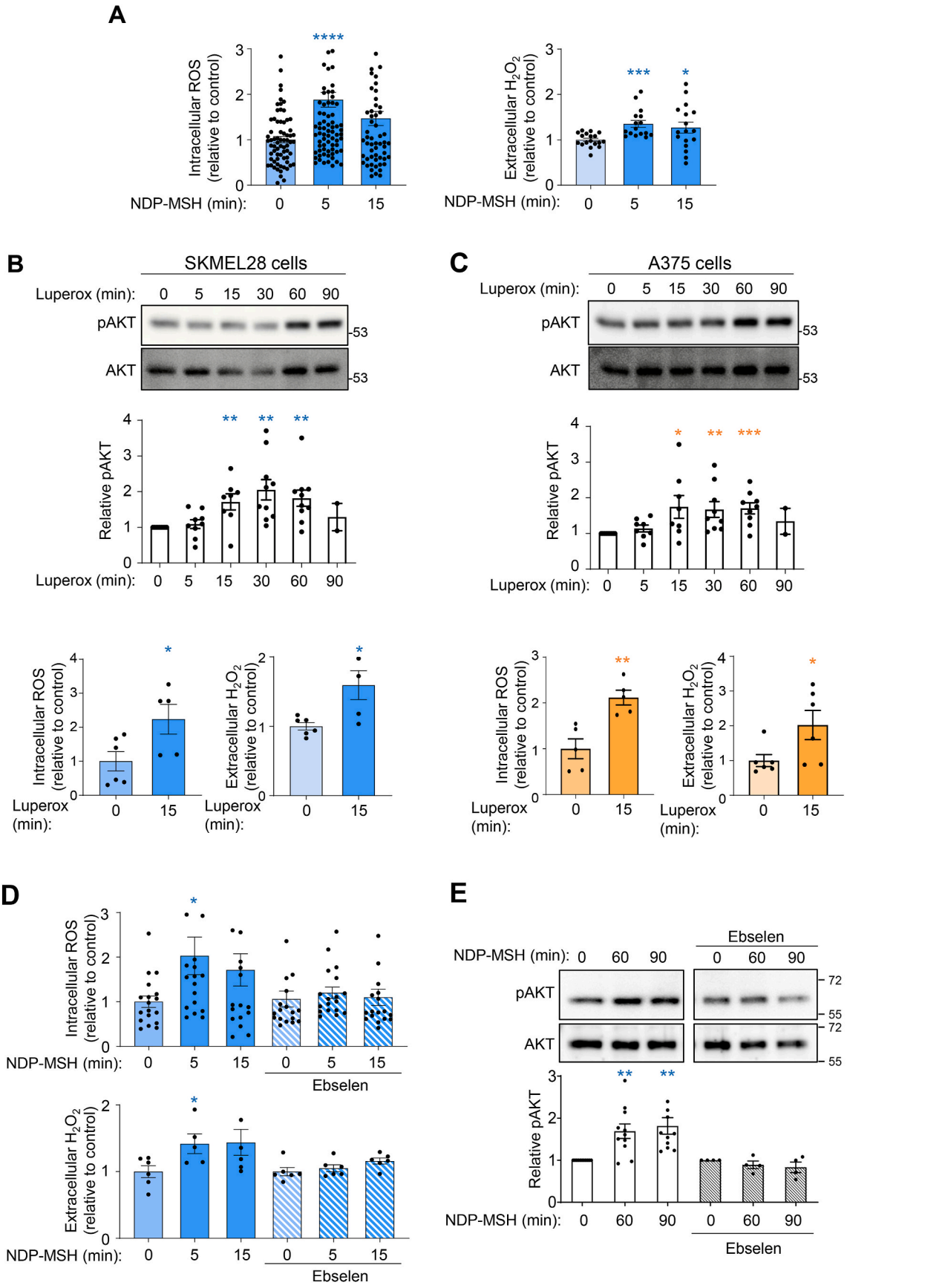

(caption on next page)

Fig. 2. Involvement of ROS in AKT activation downstream of varMC1R. **(A) NDP-MSH-induced ROS production.** SKMEL28 cells were stimulated with 10 nmol/L NDP-MSH for the times shown, then intracellular (left panel) and extracellular (H_2O_2, right) ROS were quantified with H_2DCFDA and Amplex red, respectively. Data represent the mean fold-change of ROS-induced fluorescence normalized to the untreated control. **(B and C) Kinetics of AKT activation by Luperox**. SKMEL28 **(B)** or A375 **(C)** cells were serum-starved and challenged with Luperox (80 μmol/L) for the times shown. Representative immunoblots (top panel) and quantification of the intensity of the pAKT signal relative to the control (middle panel) are shown as mean ± SEM. Total AKT was used as loading control and for normalization. Intracellular and extracellular (H_2O_2) ROS levels in Luperox-treated cells (80 μmol/L, 15 min), determined as above, are also shown (bottom panel). **(D) Inhibition of ROS production and (E) AKT activation by the antioxidant ebselen in SKMEL28 HMCs.** Cells were pretreated with ebselen (40 μmol/L, 12h) prior to NDP-MSH stimulation (100 nmol/L) for the times shown, then ROS (**D**) and pAKT levels (**E**) were analyzed as above. (For interpretation of the references to color in this figure legend, the reader is referred to the Web version of this article.)

significantly protected by NDP-MSH from Luperox-induced guanine oxidation (Supplementary Fig. 1C, right panel). However, the accumulation of oxidative DNA damage caused by Luperox remained detectable, although smaller than in MC1R-KO cells, indicating a significant but less effective protection downstream of varMC1R compared with wtMC1R. These results confirmed that the protective effect of the melanocortin observed in HMCs was fully dependent on expression of MC1R and that, as suggested by the data obtained in A375 and SKMEL28 HMCs, varMC1R signaling was able to afford protection against oxidative DNA damage.

3.2. ROS-mediated activation of AKT downstream of varMC1R

Since the results presented above also showed that AKT activation was required for the DNA-protective action of varMC1R, we next analyzed the pathway leading from varMC1R to AKT. Our group showed previously that hormone-stimulated varMC1R transactivates the cKIT tyrosine kinase receptor in cKIT-expressing HMCs [42], which could conceivably account for AKT activation. However, this was ruled out by lack of cKIT expression in A375 and SKMEL28 cells (Supplementary Fig. 2A). On the other hand, ROS-mediated redox signaling can activate a number of protein kinases including AKT [43,44]. Moreover, certain physiological actions of GPCRs are mediated by ROS acting as second messengers, and various signaling pathways linking GPCRs and activation of ROS-generating NADPH oxidases have been described [45]. Accordingly, we investigated a possible role of ROS in AKT activation downstream of varMC1R. First, we measured ROS levels in SKMEL28 and A375 cells stimulated with NDP-MSH by using two complementary methods. Intracellular ROS were determined with the cell-permeant probe H_2DCFDA, and H_2O_2 in the extracellular medium was also investigated using the Amplex Red reagent. This reagent consists of the cell-impermeant dye Amplex UltraRed which, in the presence of extracellular H_2O_2, is oxidized to a fluorescent product by a peroxidase provided by the reagent. Both in SKMEL28 cells (Fig. 2A) and in A375 cells (Supplementary Fig. 2B), we found a rapid increase in intracellular ROS estimated with H_2DCFDA, as well as a significant increase in extracellular H_2O_2 detected with Amplex Red occurring with a similar kinetics. Therefore, ROS could act as second messengers downstream of MC1R.

Next, varMC1R HMCs were pulsed with a lower concentration of Luperox (80 μmol/L), that should not decrease cell viability since the higher concentration used to generate DNA damage did not cause significant changes in proliferation of A375 or SKMEL28 cells [36]. Treatment with exogenous ROS stimulated AKT efficiently in SKMEL28 and A375 cells (Fig. 2B and C). Importantly, the concentration of exogenous Luperox used in this experiment increased intra- and extracellular ROS to levels comparable with those achieved by NDP-MSH stimulation (Fig. 2A, B and 2C). To analyze whether NDP-MSH-induced intracellular ROS were indeed responsible for AKT activation downstream of MC1R, we used the antioxidant ebselen, which blocks ROS-dependent processes. We treated varMC1R HMCs with ebselen (40 μmol/L) before and during the NDP-MSH challenge and next, we analyzed ROS concentrations and AKT activation. Both agonist-induced ROS production and AKT activation were blocked by the antioxidant treatment (Fig. 2D and E and Supplementary Figs. 2C and 2D).

Overall, these data showed that i) stimulation of varMC1R in two different HMC lines triggered a rapid and transient increase in ROS followed by a slower AKT activation, ii) increasing ROS levels by addition of Luperox to the culture medium stimulated AKT and iii) blocking ROS production downstream of varMC1R also blocked AKT activation. Accordingly, intracellular ROS fulfilled the criteria for second messengers mediating AKT activation downstream of varMC1R.

3.3. NADPH oxidase (NOX) activation downstream of varMC1R

Within melanocytes and HMCs, ROS can be generated by various mechanisms including excitation of endogenous photosensitizers by solar radiation, as byproducts of the metabolic activity of melanosomes and mitochondria or by certain enzymatic reactions. The NADPH oxidase (NOX) family enzymes are a major source of ROS acting as second messengers in GPCR-initiated signal transduction [45–48]. Of note, in addition to its ROS-scavenging properties, ebselen is also an inhibitor of several NOX isoenzymes [49,50]. Therefore, NDP-MSH might stimulate ROS production via activation of at least one enzyme of this family. It is worth noting that NOX1 is expressed in the skin [51], is regulated downstream of several GPCRs [52] and is involved in UVA- and UVB-induced signaling in human keratinocytes [52–54]. Moreover, by Western blot analysis, we found that both SKMEL28 and A375 cells expressed NOX1 (Supplementary Fig. 3A). Accordingly, we analyzed the effects on ROS production downstream of varMC1R of DPI, a low specificity general NOX inhibitor, and GKT137831, a potent NOX1 inhibitor that can also inhibit NOX4 [50,51]. Cells were pretreated with these compounds before stimulation with NDP-MSH, and ROS production was analyzed. Both agents blocked ROS production in HMCs (Fig. 3A and Supplementary Fig. 3B). Moreover, AKT activation by NDP-MSH was also abolished by pharmacological inhibition of NOX enzymes in SKMEL28 (Fig. 3B) and A375 (Supplementary Fig. 3C) cells. To further support the involvement of NOX1 in AKT activation downstream of varMC1R, we attempted to knockdown NOX1 expression with specific siRNA. The siRNA treatment yielded modest reductions of NOX1 levels around 30% in SKMEL28 cells (Fig. 3C). Attempts to achieve a stronger downregulation of NOX1 with other commercial oligonucleotides were unsuccessful (not shown). Nevertheless, partial repression of NOX1 reduced the ability of NDP-MSH to increase the phosphorylation of AKT throughout a 120 min stimulation of SKMEL28 cells, as no statistically significant differences were observed during the time course of the experiment, even though a trend towards increased AKT activity could still be seen (Fig. 3D). Conversely, as expected, AKT phosphorylation increased significantly following treatment with the hormone in cells treated with a control non-targeting siRNA. Similar results were obtained with A375 cells (Fig. 3E and F). Therefore, our results were consistent with the involvement of NOX1 in activation of AKT downstream of varMC1R.

Since AKT activation was required for NDP-MSH-mediated protection against oxidative lesions such as 8-oxodG and DNA strand breaks [36], NOX inhibition should also block the genoprotective action of NDP-MSH DNA damage in cells of varMC1R genotype. To verify this point, we abolished ROS generation downstream of MC1R with NOX inhibitors or with ebselen and we assessed 8-oxodG levels in Luperox-stressed cells. Treatment with ebselen was performed before and during MC1R stimulation with NDP-MSH, but ebselen was removed

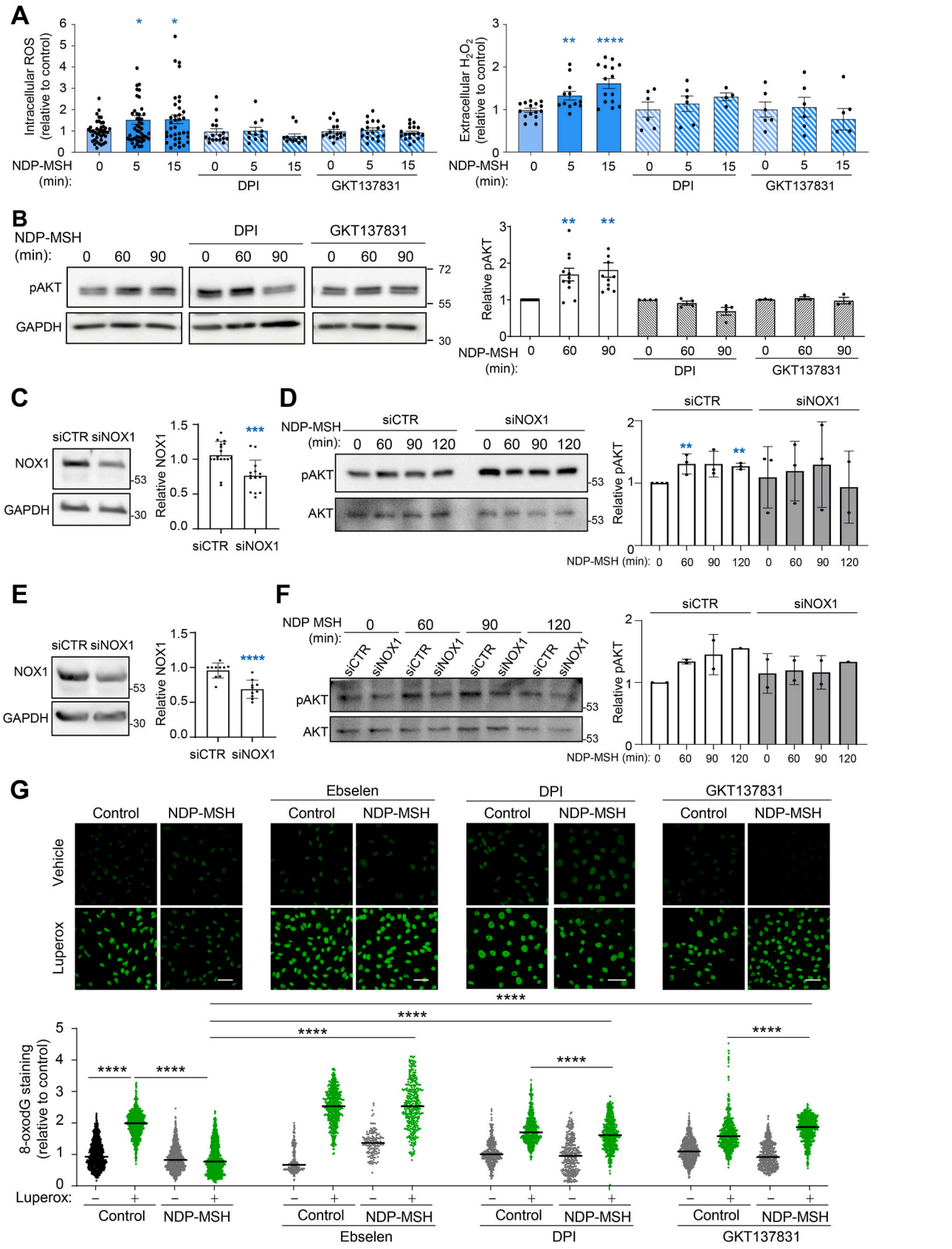

(caption on next page)

Fig. 3. Inhibition of NOX prevents NDP-MSH-induced ROS generation, AKT activation and reduction of DNA oxidative damage in varMC1R melanoma cells. **(A) ROS production.** SKMEL28 cells were pretreated with (from left to right) DPI (25 μmol/L, 2h) or GKT137831 (50 μmol/L, 2h) prior to NDP-MSH stimulation (100 nmol/L) for the times shown. Then, intracellular (left) and extracellular (H_2O_2, right) ROS levels were assessed. Histograms showing the mean fold-change of ROS levels. **(B) AKT activation.** Cells were treated as in panel A and levels of the active pAKT form were analyzed by Western blot. GAPDH was used as loading control. Quantification of the intensity of pAKT signal relative to the control is shown below. **(C) Partial knockdown of NOX1 in SLMEL28 cells.** Cells were treated with control nontargeting (siCTR) or NOX1-directed (siNOX1) siRNA, and the levels of NOX1 were compared by Western blot. A representative blot is shown on the left, with the quantification on the right. **(D) Impaired AKT activation upon siRNA-mediated repression of NOX1.** Cells treated with siCTR or siNOX1 were stimulated with NDP-MSH for the times shown and the levels of the active pAKT form were analyzed by Western blot. Total AKT was used as loading control. Quantification of the intensity of pAKT signal relative to the control is also shown. (**E and F)** Same as in panels C and D, except that A375 cells were used**. (G) NOX-dependent protection against Luperox-induced oxidative DNA damage.** SKMEL28 cells were pretreated with the antioxidant ebselen (40 μmol/L, 12h) or with the NOX inhibitors DPI (25 μmol/L, 2h) or GKT137831 (50 μmol/L, 2h) before stimulation with NDP-MSH (100 nmol/L, 24h). Then, cells were challenged with Luperox (15 nmol/L, 30 min), fixed and immunostained for 8-oxodG. Representative confocal images are shown (bar size: 50 μm). The bar graph below the confocal images presents the quantitative analysis of nuclear 8-oxodG fluorescence intensity, normalized to the average signal of the untreated controls.

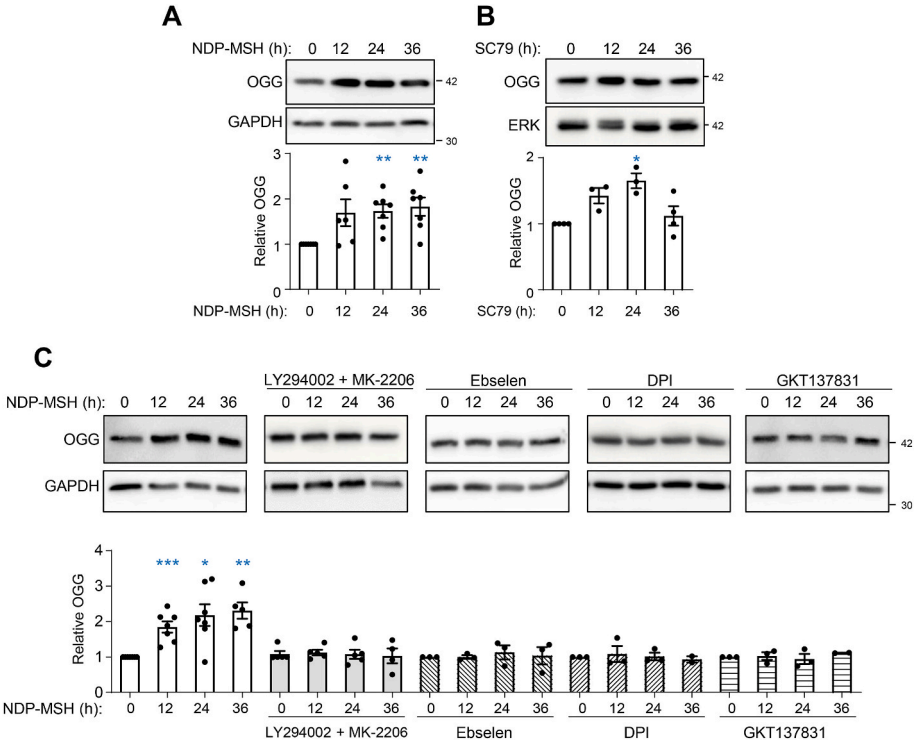

Fig. 4. Induction of the rate-limiting BER enzyme OGG downstream of varMC1R in SKMEL28 melanoma cells. **(A) Increased OGG expression in NDP-MSH-stimulated melanoma cells.** SKMEL28 cells were stimulated with 100 nmol/L NDP-MSH for the times shown, and expression of OGG was estimated by Western blot. GAPDH was used as control for loading. The graph bar shows the quantification of the blots, with all values normalized to the intensity of the OGG signal corresponding to the untreated controls. **(B) Effect of AKT activation in OGG expression.** SKMEL28 cells were treated with SC79 (10 μg/ml) for the times shown, then analyzed for OGG expression as in panel A. **(C) Effect of inhibition of AKT or NOX on NDP-MSH-induced OGG expression.** SKMEL28 cells were stimulated with NDP-MSH (100 nmol/L) for the times shown with or without pretreatment with (from left to right) a combination of LY294002 (20 μmol/L, 2h) and MK-2206 (5 μmol/L, 2h), ebselen (40 μmol/L, 12h), DPI (25 μmol/L, 2h) or GKT137831 (50 μmol/L, 2h), as indicated. In all conditions, the kinetics of OGG induction was followed by Western blot as in (A). For all panels, representative immunoblots (top) out of at least 3 independent experiments (bottom) are shown.

from the medium during the oxidative pulse. In these conditions, ebselen should interfere with NDP-MSH actions while allowing for a normal oxidative challenge. Ebselen, DPI and GKT137831 abolished varMC1R-dependent clearance of 8-oxodG in HMCs (Fig. 3G and Supplementary Fig. 4A). DPI also abolished clearance of SBs as assessed by comet assay (Supplementary Fig. 4B).

3.4. NOX- and AKT-dependent induction of BER pathway by varMC1R

So far, we have shown that stimulation of a NOX isoenzyme, most likely NOX1, downstream of varMC1R afforded AKT-dependent protection against oxidative DNA lesions. Since the BER pathway mediates clearance of 8-oxodG and SBs, we hypothesized that this pathway should be involved in the protective action of varMC1R. Thus, we analyzed the induction of 8-oxoguanine DNA glycosylase/AP lyase (OGG) by NDP-MSH in varMC1R melanoma cells. OGG is the BER enzyme responsible for the rate-limiting recognition and excision of 8-oxodG. SKMEL28 and A375 cells were stimulated with the MC1R agonist for up to 36 h and we determined OGG expression by Western blot. NDP-MSH triggered a statistically significant induction of OGG (Fig. 4A and Supplementary Fig. 5A). Moreover, we confirmed that AKT activation in varMC1R was sufficient to trigger OGG induction by treating cells with SC79 (Fig. 4B and Supplementary Fig. 5B).

Although these results supported a varMC1R → NOX→ ROS → AKT → BER pathway, a formal link between AKT or NOX activation and induction of BER by NDP-MSH remained to be established. Thus, we blocked AKT activation with LY94002 and MK-2206, and ROS-dependent signaling with ebselen or NOX inhibitors and we assessed OGG induction in NDP-MSH-stimulated cells. Inhibition of AKT or NOX-mediated ROS signaling effectively prevented OGG induction in SKMEL28 (Fig. 4C) and A375 cells (Supplementary Fig. 5C).

To further extend these results, we checked the induction of another

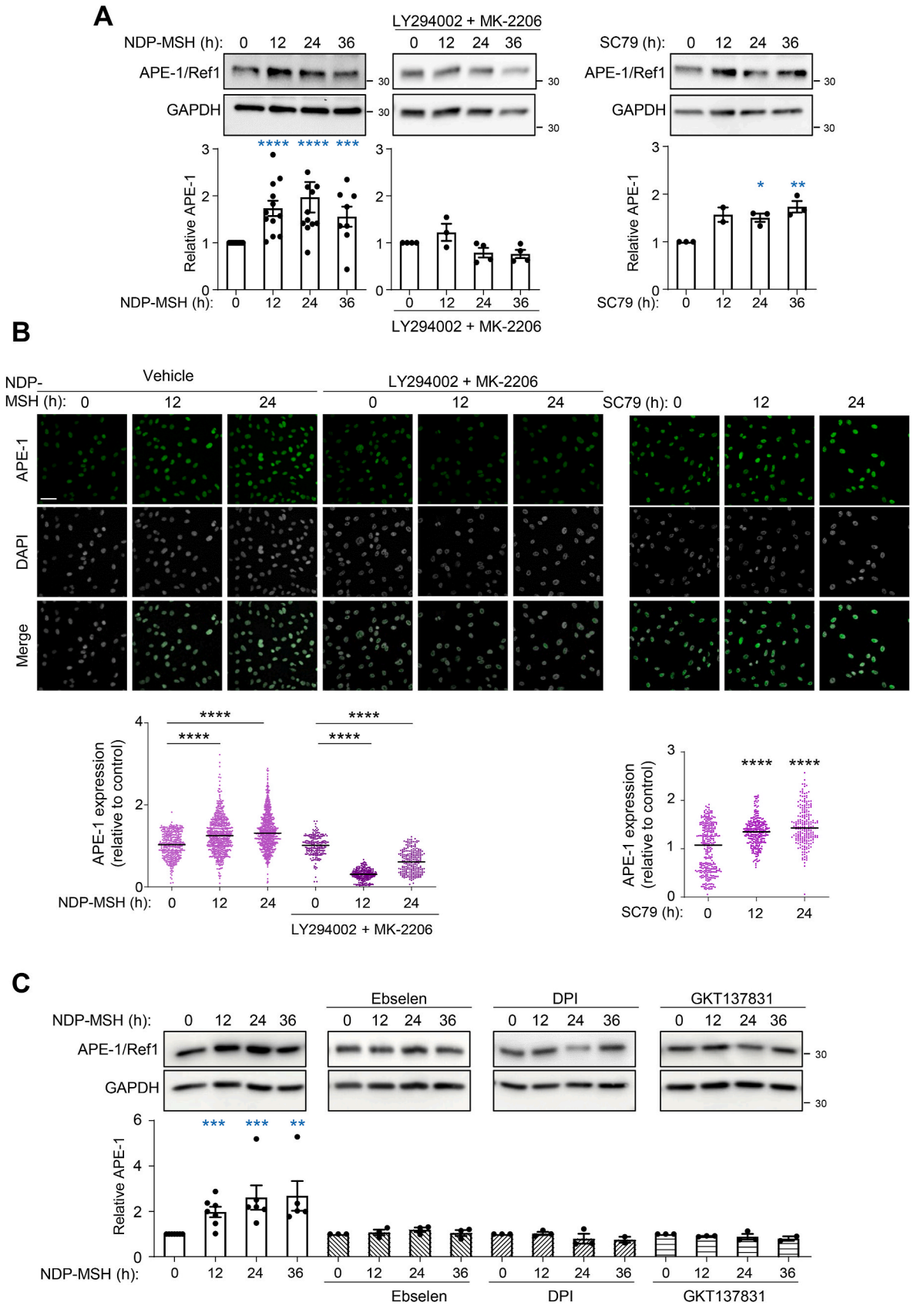

(caption on next page)

Fig. 5. Induction of APE-1/Ref-1 downstream of varMC1R in SKMEL28 melanoma cells. **(A) AKT dependent induction of APE-1/Ref-1 in NDP-MSH treated cells.** Cells were stimulated for the times shown with NDP-MSH (100 nmol/L), without (left) or with pretreatment with a combination of LY294002 (20 μmol/L, 2h) and MK-2206 (5 μmol/L, 2h) (middle), or treated with SC79 (10 μg/ml) (right) and analyzed for APE-1/Ref-1 expression by Western blot. Representative immunoblots (top) and quantification (bottom) are shown ($n \geq 3$). GAPDH signal was used as loading control. Values were normalized to the 0 time-point. **(B) Confocal microscopy analysis of APE-1/Ref-1 expression.** Cells were treated as in panel A, fixed, immunostained for APE-1/Ref1 and images were taken with a confocal microscope. Representative confocal images (top, bar size: 50 μm) and their quantification (bottom) are shown. For quantification, at least 300 nuclei were analyzed ($n = 3$). **(C) ROS- and NOX-dependent induction of APE-1/Ref-1 in NDP-MSH-treated cells.** SKMEL28 cells were stimulated with NDP-MSH for the times shown with or without pretreatment with ebselen or the NOX inhibitors DPI and GKT137831 as in Fig. 4C. The kinetics of induction of APE-1/Ref-1 was followed by Western blot. GAPDH was used as loading control. Values were normalized to the 0 time-point. Representative immunoblots (top), and quantification of at least 3 independent experiments (bottom) are shown.

key enzyme of the BER pathway, APE-1/Ref1, downstream of varMC1R. This enzyme creates a nick in the phosphodiester backbone of the abasic site generated by OGG or other DNA glycosylases, which is further processed to repair the lesion [56]. APE-1//Ref1 expression was significantly augmented by NDP-MSH in varMC1R cells. This induction was blocked by AKT inhibition with LY294002 and MK-2206 and was mimicked by the AKT agonist SC79 (Fig. 5A and Supplementary Fig. 6A). We confirmed these findings by APE-1/Ref1 immunostaining (Fig. 5B and Supplementary Fig. 6B). The intensity of the APE-1/Ref-1 signal increased significantly after stimulation with NDP-MSH or SC79, and the NDP-MSH-mediated increase was blocked by inhibition of AKT (Fig. 5B and Supplementary Fig. 6B). Finally, the involvement of NOX in induction of APE-1/Ref1 was further confirmed by Western blot analysis of control cells and cells treated with ebselen or NOX inhibitors (Fig. 5C and Supplementary Fig. 6C).

3.5. cAMP-dependent, NOX/AKT-independent induction of the BER pathway downstream of wtMC1R

Others [34] and we [36] have shown that wtMC1R activity affords protection against oxidative stress and oxidative DNA damage in a cAMP-dependent manner. We wanted to confirm that this protective action of wtMC1R also relied on induction of BER enzymes and was dependent on cAMP. To this end, we used HBL HMCs cells expressing functional MC1R and displaying strong activation of cAMP signaling upon stimulation with NDP-MSH [42]. Treatment of HBL cells with NDP-MSH induced OGG and APE-1/Ref-1 (Fig. 6A), consistent with previous findings in normal human melanocytes [34]. This induction was quantitatively like the one observed in varMC1R HMCs, but the signaling pathway was different. Indeed, in HBL cells, NDP-MSH not only failed to achieve a rapid and transient increase in ROS, but rather triggered a slower decrease in the concentration of intracellular ROS (Fig. 6B). Moreover, NDP-MSH did not increase pAKT levels, thus demonstrating that wtMC1R did not activate AKT in these cells, at least within the time course of our experiment (Fig. 6C). Therefore, neither NOX nor AKT were activated downstream of wtMC1R. In agreement with this conclusion, induction of OGG and APE-1/Ref-1 by NDP-MSH was not blocked by GKT137831 but was effectively prevented by DDA, an inhibitor of adenylyl cyclase (AC), the enzyme responsible for cAMP synthesis (Fig. 6D).

4. Discussion

Var*MC1R* alleles associated with the RHC phenotype are major genetic determinants of melanoma risk [20–22]. This association is most often believed to rely on hypomorphic cAMP signaling, which leads to biosynthesis of photosensitizing pheomelanic pigments and impairs the DNA repair-inducing activity of wtMC1R [11]. However, although frequent melanoma-associated MC1R variants such as R151C do not stimulate efficiently cAMP synthesis [14,15], they are able to activate not only the ERK pathway comparably to wtMC1R [14,35] but also AKT signaling, leading to significant protection against DNA SBs generated by oxidative stress [36]. Therefore, the signaling properties of common melanoma-associated *MC1R* variants are complex and further study of the cellular responses downstream of varMC1R, particularly as related with protection of DNA, remains important to understand the molecular bases of their association with increased melanoma risk.

UVR promotes DNA injury by several mechanisms. Direct absorption of energetic UVB photons leads to formation of pyrimidine dimers. These are cleared by the nucleotide excision repair (NER) pathway [57], but when unrepaired, they cause the most common somatic mutations in melanoma, the C → T or CC → TT transitions corresponding to an UVR mutational signature [58,59]. On the other hand, UVA leads to ROS-mediated oxidation of DNA bases and to single strand DNA breaks. These lesions are most often repaired by the BER pathway [60]. The genoprotective action of MC1R by cAMP-dependent induction of NER has been relatively well analyzed [31], but data on modulation by MC1R of BER-dependent oxidative DNA damage repair remain scarce [34]. Yet the pheomelanin pigments characteristic of carriers of varMC1R are believed to act as photosensitizers that enhance UVR-induced ROS production and oxidative DNA damage [1]. Moreover, pheomelanins also promote oxidative stress and ultimately melanomagenesis by UVR-independent mechanisms [61–63]. In this line, Mitra et al. showed that mice with a red/yellow fur bearing a conditional *BRAF*^{V600E} mutant allele developed invasive melanoma at higher rates than albino mice with the same genetic background even in the absence of UVR [64]. Thus, oxidative stress is considered to contribute to melanomagenesis, particularly in people with pheomelanic pigmentation [9]. Accordingly, we focused on protection against oxidative DNA lesions in cells of var*MC1R* genetic background.

The results summarized above showed that stimulation of varMC1R in two different melanoma cells lines induced the expression of OGG and APE-1/Ref-1, the rate-limiting enzymes for BER-mediated clearance of 8-oxodG. Although we analyzed enzyme levels rather than enzymatic activity, it is reasonable to assume that the observed increase of OGG and APE1 abundance in varMC1R cells treated with NDP-MSH enhanced their activity and hence stimulated the BER pathway, particularly in the light of the observed reduction of 8-oxodG burden. These results are in line with the previously reported increase of DNA strand break repair in HMCs of varMC1R genotype treated with NDP-MSH [36], although a causal link between induction of the rate-limiting BER enzymes OGG and APE1 on one hand, and reduction of the 8-oxodG burden in varMC1R melanoma cells undergoing oxidative stress remains to be formally established. Concerning the pathway leading to induction of BER downstream of varMC1R, a combination of genetic and pharmacological approaches strongly suggested that BER induction relied on AKT activity. Moreover, NDP-MSH induced a transient increase of ROS production, and AKT activation was mimicked by treatment with exogenous ROS and prevented by a ROS scavenger. Overall, these data supported a varMC1R → NOX → ROS → AKT → BER pathway.

Although we have not identified unequivocally the NOX isoenzyme downstream of varMC1R, NOX1 or NOX4 were the most likely candidates, because the genoprotective responses downstream varMC1R were blocked by GKT137831, a specific dual inhibitor of these isoenzymes [50]. Both NOX1 and NOX4 are expressed in the skin [51,65], and NOX1 expression is high in human melanoma cells. Whereas NOX1 is regulated by several GPCRs [52], NOX4 is constitutively active and often considered a transcriptionally regulated protein [47]. This type of regulation would hardly be compatible with the rapid activation of ROS production observed here. Moreover, the activation of AKT required for BER

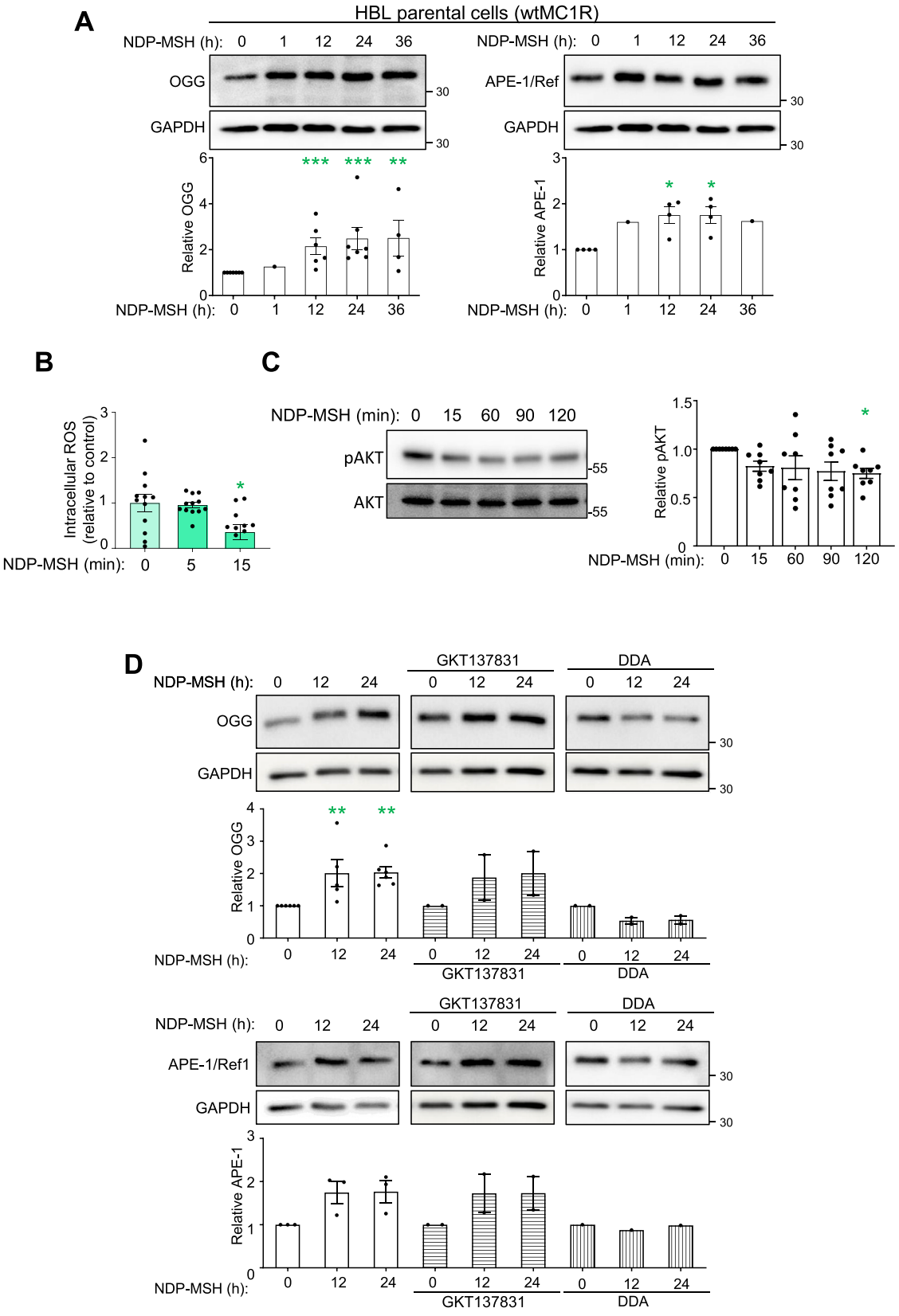

(caption on next page)

Fig. 6. (A) Induction of BER enzymes by activation of wtMC1R. (A) HBL melanoma cells were stimulated with 100 nmol/L NDP-MSH for the indicated times. Expression of OGG (left) and APE-1/Ref-1 (right) was estimated by Western Blot. Representative immunoblots (top) and quantification of 3 independent experiments (bottom) are shown for each BER enzyme. ERK2 or GAPDH were used as loading control and the intensity signals were normalized to the 0 time-point. **(B) Lack of ROS production upon stimulation of wtMC1R with NDP-MSH.** HBL cells were serum-deprived for at least 3 h, then stimulated with NDP-MSH (100 nmol/L). ROS levels were measured with the H_2DCFDA assay. Data represent the mean fold-change of ROS-induced fluorescence and are given as mean ± SEM (n = 3 with at least 3 replicate wells for each experiment). **(C) Lack of AKT activation in wtMC1R HBL cells stimulated with NDP-MSH.** HBL cells were stimulated with NDP-MSH for the times shown. Representative immunoblots (top) and their quantification using GAPDH as loading control (bottom) are shown. Values were normalized to the 0 time-point. **(D) Effect of NOX and adenylyl cyclase inhibition on MSH-induced expression of BER enzymes.** HBL melanoma cells, with or without pre-treatment with the NOX1/4 inhibitor GKT137831 (50 μmol/L, 2h) or the adenylyl cyclase inhibitor 2',5'-dideoxyadenosine (DDA, 2.5 mmol/L, 2h), were stimulated with 100 nmol/L NDP-MSH for the indicated times. Expression of OGG1 (top) and APE-1/Ref-1 (bottom) were estimated by Western Blot. Representative immunoblots and the quantification of at least 2 independent experiments using GAPDH signal as loading control are shown. The values were normalized to the 0 time-point.

induction downstream of varMC1R was impaired by siRNA-mediated partial knockdown of NOX1. Of note, keratinocytes produce ROS in a NOX1-dependent fashion when irradiated with either UVB [52–54,65–67] or UVA [68], and the resulting increase in intracellular ROS has been reported to modulate DNA damage repair [65]. NOX1 is a multimeric enzyme whose activity is tightly controlled through the association of several subunits, including NOXA1 and NOXO1. cAMP has been shown to inhibit NOX1 by a mechanism involving PKA-dependent phosphorylation of NOX activator 1 (NOXA1), leading to its dissociation from the active NOX1 complex [68,69]. Interestingly, in HBL cells stimulation of wtMC1R with NDP-MSH increased intracellular cAMP levels repair [36] and reduced intracellular ROS levels (Fig. 6B). Therefore, NOX1 might be the specific NOX isoenzyme responsible for AKT activation downstream of varMC1R.

On the other hand, ROS-mediated stimulation of AKT downstream of varMC1R could rely on activation of an upstream kinase or on inhibition of a phosphatase. Notably, the PTEN phosphatase, which blocks AKT stimulation, is inactivated by H_2O_2-mediated oxidation of specific Cys residues [70]. ROS-dependent inactivation of PTEN might increase the level of phosphorylated active AKT with a slower kinetics compatible with our data. Interestingly, another mechanism linking varMC1R and AKT signaling has been described [71], whereby exposure of melanocytes to UVR triggered association of PTEN with wtMC1R, but not with varMC1R. The wtMC1R-PTEN interaction protected PTEN from ubiquitin-dependent degradation, thus promoting AKT inactivation. Therefore, in varMC1R melanocytes, increased proteolysis of PTEN and ROS-dependent inactivation of the residual enzyme could cooperate to increase AKT activity, particularly following exposure to UVR. Conversely, in wtMC1R melanocytes, PTEN would be protected from proteolytic degradation by its interaction with the receptor, and from oxidative inactivation by the potent cAMP response elicited by melanocortin agonists which is expected to inhibit NOX1-mediated production of ROS. In agreement with this scenario, others and we have reported that cAMP inhibits PI3K/AKT signaling in melanoma cells [36,72–74]. In any case, the available evidence suggests that a wtMC1R background should be associated with low AKT activity. Conversely, a varMC1R background would allow for higher AKT activity [71] leading to upregulation of BER. This would enable cAMP-independent repair of oxidative DNA damage to promote survival under conditions of chronic oxidative stress typically present in pheomelanic cells.

Since 8-oxodG pairs with adenine rather than cytosine during replication [9], unrepaired 8-oxodG promotes the G → T transversion that dominates signature 18 from the COSMIC catalogue of mutational signatures (cancer.sanger.ac.uk/signatures/). Yet, no evidence for significant association of this signature with human melanoma has been found, despite extensive analyses [7,59]. This suggests that oxidative mutagenesis is not a major contributor to melanomagenesis [9], despite the pro-oxidant environment and increased oxidative stress in the pheomelanic skin of individuals with varMC1R. The significant induction of BER downstream of varMC1R reported here provides a possible explanation for this paradox and underscores the question of the actual molecular basis of the association of varMC1R with risk of melanoma. In this respect, the vast majority of UVR lesions are pyrimidine dimers that can be cleared by NER but, if unrepaired, promote the C → T transitions overwhelmingly dominating the mutational landscape of melanomas [2,6,7,75]. Therefore, the well-established impairment of NER induction downstream of varMC1R compared with wtMC1R [31,32,76] might be a more important factor in melanomagenesis than UVA-induced oxidative DNA damage, particularly since the UVA component of solar radiation has been reported to decrease NER efficiency (reviewed in Ref. [9]). On the other hand, a significant upregulation of both BER and AKT-dependent pro-survival signaling may help pheomelanic varMC1R melanocytes to cope with continuous oxidative stress and to avoid DNA damage-induced apoptosis. Of note, *BRAF* mutations are frequent in nevi [77], but these benign lesions can remain stable for long times. This shows that mutant *BRAF* is not sufficient to cause malignant transformation, most likely due to its ability to promote oncogene-induced senescence. It has been shown that activation of PI3K/AKT signaling abrogates oncogene-induced senescence in melanocytes and serves as a rate-limiting event in the progression of nevi to melanomas [71,78]. Moreover, early reports demonstrated that the effects of αMSH on proliferation and adhesion to fibronectin are different in cells of variant compared with wildtype *MC1R* genotype [79]. Therefore, several mechanisms can contribute to the increased melanoma risk of carriers of varMC1R, independently of pigmentary effects or accumulation of oxidative DNA damage. In summary, our findings do not oppose, but rather complement, the current paradigm explaining increased melanoma risk in carriers of varMC1R in terms of deficient induction of DNA repair. Indeed, even if MC1R variants can stimulate the BER pathway, they are most likely less effective than wtMC1R in stimulating NER and maybe other repair pathways. In fact, the available literature strongly suggests that the association of varMC1R and higher melanoma risk is multifactorial and complex, possibly involving factors not only related with pigmentary effects and DNA repair, but also with differential activation of AKT signaling and changes in cell shape and motility. In any case, the observations reported here underscore the complexity of this association and highlight the relevance to further investigation on these topics for the rational development of strategies to correct defective varMC1R responses for efficient photoprotection and melanoma prevention in fair-skinned individuals [80].

Sources of funding

This work was supported by Instituto de Salud Carlos III (ISCIII), through the project PI22/00404 and co-funded by the European Union (to C.J-C. and J.C.G.-B.). M Castejón-Griñán holds a postdoctoral research contract from the AECC Scientific Foundation (Grant Number POSTD235118CAST). Sonia Cerdido holds a FPI predoctoral fellowship from the University of Murcia and José Sánchez-Beltrán is recipient of a PFIS 2023 contract (FI23/00090) from the "Acción Estratégica en Salud, Ministerio de Ciencia, Innovación y Universidades, Instituto de Salud Carlos III", co-financed by the European Union through the FSE + fund.

CRediT authorship contribution statement

María Castejón-Griñán: Writing – review & editing, Methodology,

Investigation, Formal analysis, Conceptualization. **Sonia Cerdido:** Writing – review & editing, Investigation, Formal analysis. **José Sánchez-Beltrán:** Writing – review & editing, Investigation, Formal analysis. **Ana Lambertos:** Writing – review & editing, Investigation, Formal analysis. **Marta Abrisqueta:** Writing – review & editing, Investigation, Formal analysis. **Cecilia Herraiz:** Writing – review & editing, Methodology. **Celia Jiménez-Cervantes:** Writing – review & editing, Supervision, Project administration, Methodology, Funding acquisition, Formal analysis, Conceptualization. **José Carlos García-Borrón:** Writing – review & editing, Writing – original draft, Supervision, Funding acquisition, Formal analysis, Data curation, Conceptualization.

Declaration of competing interest

None of the authors have any competing interest to declare.

Data availability

Data will be made available on request.

Acknowledgements

We thank Prof G Ghanem, from the Free University of Brussels for gift of human melanoma cell lines.

Appendix A. Supplementary data

Supplementary data to this article can be found online at https://doi.org/10.1016/j.redox.2024.103135.

References

[1] R.M. Slominski, et al., Melanoma, Melanin, and Melanogenesis: the Yin and Yang Relationship, vol. 12, 2022, p. 1.
[2] J. D'Orazio, S. Jarrett, A. Amaro-Ortiz, T. Scott, UV radiation and the skin, Int. J. Mol. Sci. 14 (2013) 12222–12248.
[3] C. Kielbassa, L. Roza, B. Epe, Wavelength dependence of oxidative DNA damage induced by UV and visible light, Carcinogenesis 18 (1997) 811–816.
[4] T. Douki, The variety of UV-induced pyrimidine dimeric photoproducts in DNA as shown by chromatographic quantification methods, Photochem. Photobiol. Sci. 12 (2013) 1286–1302.
[5] J. Cadet, S. Mouret, J.-L. Ravanat, T. Douki, Photoinduced damage to cellular DNA: direct and photosensitized reactions, Photochem. Photobiol. 88 (2012) 1048–1065.
[6] E.D. Pleasance, et al., A comprehensive catalogue of somatic mutations from a human cancer genome, Nature 463 (2010) 191–196.
[7] N.K. Hayward, et al., Whole-genome landscapes of major melanoma subtypes, Nature 545 (2017) 175–180.
[8] J. Cadet, T. Douki, J.-L. Ravanat, Oxidatively generated damage to cellular DNA by UVB and UVA radiation, Photochem. Photobiol. 91 (2015) 140–155.
[9] T. Douki, Oxidative stress and genotoxicity in melanoma induction: impact on repair rather than formation of DNA damage? Photochem. Photobiol. 96 (2020) 962–972.
[10] J.C. Garcia-Borron, B.L. Sanchez-Laorden, C. Jimenez-Cervantes, Melanocortin-1 receptor structure and functional regulation, Pigm. Cell Res. 0 (2005) 051103015727002.
[11] J.C. Garcia-Borron, Z. Abdel-Malek, C. Jimenez-Cervantes, MC1R, the cAMP pathway, and the response to solar UV: extending the horizon beyond pigmentation, Pigment Cell Melanoma Res 27 (2014) 699–720.
[12] C. Herraiz, I. Martínez-Vicente, V. Maresca, The α-melanocyte-stimulating hormone/melanocortin-1 receptor interaction: a driver of pleiotropic effects beyond pigmentation, Pigment Cell Melanoma Res 34 (2021) 748–761.
[13] C. Herraiz, J.C. Garcia-Borron, C. Jiménez-Cervantes, C. Olivares, MC1R signaling. Intracellular partners and pathophysiological implications, Biochim. Biophys. Acta (BBA) - Mol. Basis Dis. (2017), https://doi.org/10.1016/j.bbadis.2017.02.027.
[14] C. Herraiz, C. Jimenez-Cervantes, P. Zanna, J.C. Garcia-Borron, Melanocortin 1 receptor mutations impact differentially on signalling to the cAMP and the ERK mitogen-activated protein kinase pathways, FEBS Lett. 583 (2009) 3269–3274.
[15] A. Ringholm, et al., Pharmacological characterization of loss of function mutations of the human melanocortin 1 receptor that are associated with red hair, J. Invest. Dermatol. 123 (2004) 917–923.
[16] P. Valverde, E. Healy, I. Jackson, J.L. Rees, a J. Thody, Variants of the melanocyte-stimulating hormone receptor gene are associated with red hair and fair skin in humans, Nat. Genet. 11 (1995) 328–330.
[17] J.R. Davies, et al., Inherited variants in the MC1R gene and survival from cutaneous melanoma: a BioGenoMEL study, Pigment Cell Melanoma Res 25 (2012) 384–394.
[18] Dessinioti, C., Antoniou, C., Katsambas, A. & Stratigos, A. J. Melanocortin 1 receptor variants: functional role and pigmentary associations. Photochem. Photobiol. 87, 978–987..
[19] D.L. Duffy, et al., Interactive effects of MC1R and OCA2 on melanoma risk phenotypes, Hum. Mol. Genet. 13 (2004) 447–461.
[20] C.D. Robles-Espinoza, et al., Germline MC1R status influences somatic mutation burden in melanoma, Nat. Commun. 7 (2016) 12064.
[21] P.A. Johansson, et al., Mutation load in melanoma is affected by *MC1R* genotype, Pigment Cell Melanoma Res 30 (2017) 255–258.
[22] F. Chatzinasiou, et al., Comprehensive field synopsis and systematic meta-analyses of genetic association studies in cutaneous melanoma, JNCI Journal of the National Cancer Institute 103 (2011) 1227–1235.
[23] E. Pasquali, et al., MC1R variants increased the risk of sporadic cutaneous melanoma in darker-pigmented Caucasians: a pooled-analysis from the M-SKIP project, Int. J. Cancer 136 (2015) 618–631.
[24] J.E. Hauser, et al., Melanin content and MC1R function independently affect UVR-induced DNA damage in cultured human melanocytes, Pigm. Cell Res. 19 (2006) 303–314.
[25] J.S. Palmer, et al., Melanocortin-1 receptor polymorphisms and risk of melanoma: is the association explained solely by pigmentation phenotype? Am. J. Hum. Genet. 66 (2000) 176–186.
[26] E. Tagliabue, et al., MC1R variants as melanoma risk factors independent of at-risk phenotypic characteristics: a pooled analysis from the M-SKIP project, Cancer Manag. Res. 10 (2018) 1143–1154.
[27] M.T. Bastiaens, et al., Melanocortin-1 receptor gene variants determine the risk of nonmelanoma skin cancer independently of fair skin and red hair, Am. J. Hum. Genet. 68 (2001) 884–894.
[28] A.L. Kadekaro, et al., Melanocortin 1 receptor genotype: an important determinant of the damage response of melanocytes to ultraviolet radiation, Faseb. J. 24 (2010) 3850–3860.
[29] V. Maresca, et al., MC1R stimulation by alpha-MSH induces catalase and promotes its re-distribution to the cell periphery and dendrites, Pigment Cell Melanoma Res 23 (2010) 263–275.
[30] V. Swope, Z. Abdel-Malek, MC1R: front and center in the bright side of dark eumelanin and DNA repair, Int. J. Mol. Sci. 19 (2018) 2667.
[31] E.M. Wolf Horrell, S.G. Jarrett, K.M. Carter, J.A. D'Orazio, Divergence of cAMP signalling pathways mediating augmented nucleotide excision repair and pigment induction in melanocytes, Exp. Dermatol. 26 (2017) 577–584.
[32] A.L. Kadekaro, et al., alpha-Melanocortin and endothelin-1 activate antiapoptotic pathways and reduce DNA damage in human melanocytes, Cancer Res. 65 (2005) 4292–4299.
[33] M. Bohm, et al., alpha-Melanocyte-stimulating hormone protects from ultraviolet radiation-induced apoptosis and DNA damage, J. Biol. Chem. 280 (2005) 5795–5802.
[34] A.L. Kadekaro, et al., Alpha-melanocyte-stimulating hormone suppresses oxidative stress through a p53-mediated signaling pathway in human melanocytes, Mol. Cancer Res. 10 (2012) 778–786.
[35] C. Herraiz, F. Journe, G. Ghanem, C. Jimenez-Cervantes, J.C. Garcia-Borron, Functional status and relationships of melanocortin 1 receptor signaling to the cAMP and extracellular signal-regulated protein kinases 1 and 2 pathways in human melanoma cells, Int. J. Biochem. Cell Biol. 44 (2012) 2244–2252.
[36] M. Castejón-Griñán, C. Herraiz, C. Olivares, C. Jiménez-Cervantes, J.C. García-Borrón, cAMP-independent non-pigmentary actions of variant melanocortin 1 receptor: AKT-mediated activation of protective responses to oxidative DNA damage, Oncogene 37 (2018) 3631–3646.
[37] B.L. Sanchez-Laorden, et al., Dimerization of the human melanocortin 1 receptor: functional consequences and dominant-negative effects, J. Invest. Dermatol. 126 (2006) 172–181.
[38] S. Cerdido, et al., A side-by-side comparison of wildtype and variant melanocortin 1 receptor signaling with emphasis on protection against oxidative damage to DNA, Int. J. Mol. Sci. 24 (2023) 14381.
[39] J.C. Oliveros, et al., Breaking-Cas-interactive design of guide RNAs for CRISPR-Cas experiments for ENSEMBL genomes, Nucleic Acids Res. 44 (2016) 267–271.
[40] A.P. Schuch, N.C. Moreno, N.J. Schuch, C.F.M. Menck, C.C.M. Garcia, Sunlight damage to cellular DNA: focus on oxidatively generated lesions, Free Radic. Biol. Med. 107 (2017) 110–124.
[41] H. Jo, et al., Small molecule-induced cytosolic activation of protein kinase Akt rescues ischemia-elicited neuronal death, Proc. Natl. Acad. Sci. USA 109 (2012) 10581–10586.
[42] C. Herraiz, et al., Signaling from the human melanocortin 1 receptor to ERK1 and ERK2 mitogen-activated protein kinases involves transactivation of cKIT, Mol. Endocrinol. 25 (2011) 138–156.
[43] N. Koundouros, G. Poulogiannis, Phosphoinositide 3-kinase/akt signaling and redox metabolism in cancer, Front. Oncol. 8 (2018) 160.
[44] A.V. Krylatov, et al., Reactive oxygen species as intracellular signaling molecules in the cardiovascular system, Curr. Cardiol. Rev. 14 (2018) 290–300.
[45] A. Petry, A. Görlach, Regulation of NADPH oxidases by G protein-coupled receptors, Antioxidants Redox Signal. 30 (2019) 74–94.
[46] F. Liu-Smith, R. Dellinger, F.L. Meyskens, Updates of reactive oxygen species in melanoma etiology and progression, Arch. Biochem. Biophys. 563 (2014) 51–55.
[47] A. Vermot, I. Petit-Härtlein, S.M.E. Smith, F. Fieschi, NADPH oxidases (NOX): an overview from discovery, molecular mechanisms to physiology and pathology, Antioxidants 10 (2021).

[48] F. Cattaneo, et al., Cell-surface receptors transactivation mediated by G protein-coupled receptors, Int. J. Mol. Sci. 15 (2014) 19700.
[49] S.M.E. Smith, et al., Ebselen and congeners inhibit NADPH oxidase 2-dependent superoxide generation by interrupting the binding of regulatory subunits, Chem. Biol. 19 (2012) 752–763.
[50] S. Altenhöfer, K.A. Radermacher, P.W.M. Kleikers, K. Wingler, H.H.H.W. Schmidt, Evolution of NADPH oxidase inhibitors: selectivity and mechanisms for target engagement, Antioxidants Redox Signal. 23 (2015) 406–427.
[51] G. Teixeira, et al., Therapeutic potential of NADPH oxidase 1/4 inhibitors, Br. J. Pharmacol. 174 (2017) 1647–1669.
[52] A. Glady, M. Tanaka, C.S. Moniaga, M. Yasui, M. Hara-Chikuma, Involvement of NADPH oxidase 1 in UVB-induced cell signaling and cytotoxicity in human keratinocytes, Biochem Biophys Rep 14 (2018) 7–15.
[53] S.M. Beak, Y.S. Lee, J.-A. Kim, NADPH oxidase and cyclooxygenase mediate the ultraviolet B-induced generation of reactive oxygen species and activation of nuclear factor-κB in HaCaT human keratinocytes, Biochimie 86 (2004) 425–429.
[54] A. Valencia, I.E. Kochevar, Nox1-based NADPH oxidase is the major source of UVA-induced reactive oxygen species in human keratinocytes, J. Invest. Dermatol. 128 (2008) 214–222.
[55] N. Hinz, M. Jücker, Distinct functions of AKT isoforms in breast cancer: a comprehensive review, Cell Commun. Signal. 17 (1) (2019) 1–29, 2019 17.
[56] M.L. Hegde, T. Izumi, S. Mitra, Oxidized base damage and single-strand break repair in mammalian genomes, Progress in molecular biology and translational science 110 (2012) 123–153.
[57] P.C. Hanawalt, Subpathways of nucleotide excision repair and their regulation, Oncogene 21 (2002) 8949–8956.
[58] E. Hodis, et al., A landscape of driver mutations in melanoma, Cell 150 (2012) 251–263.
[59] M.S. Lawrence, et al., Mutational heterogeneity in cancer and the search for new cancer-associated genes, Nature 499 (2013) 214–218.
[60] A.M. Whitaker, M.A. Schaich, M.S. Smith, T.S. Flynn, B.D. Freudenthal, Base excision repair of oxidative DNA damage: from mechanism to disease, Front Biosci (Landmark Ed) 22 (2017) 1493–1522.
[61] S. Lembo, et al., Light-independent pro-inflammatory and pro-oxidant effects of purified human hair melanins on keratinocyte cell cultures, Exp. Dermatol. 26 (2017) 592–594.
[62] P.M. Płonka, M. Picardo, A.T. Slominski, Does melanin matter in the dark? Exp. Dermatol. 26 (2017) 595–597.
[63] A. Napolitano, L. Panzella, G. Monfrecola, M. d'Ischia, Pheomelanin-induced oxidative stress: bright and dark chemistry bridging red hair phenotype and melanoma, Pigment Cell Melanoma Res 27 (2014) 721–733.
[64] D. Mitra, et al., An ultraviolet-radiation-independent pathway to melanoma carcinogenesis in the red hair/fair skin background, Nature 491 (2012) 449–453.
[65] H. Raad, et al., NADPH oxidase-1 plays a key role in keratinocyte responses to UV radiation and UVB-induced skin carcinogenesis, J. Invest. Dermatol. 137 (2017) 1311–1321.
[66] H. Wang, I.E. Kochevar, Involvement of UVB-induced reactive oxygen species in TGF-beta biosynthesis and activation in keratinocytes, Free Radic. Biol. Med. 38 (2005) 890–897.
[67] H.R. Rezvani, et al., Protective effects of catalase overexpression on UVB-induced apoptosis in normal human keratinocytes, J. Biol. Chem. 281 (2006) 17999–18007.
[68] P. Henri, et al., MC1R expression in HaCaT keratinocytes inhibits UVA-induced ROS production via NADPH oxidase- and cAMP-dependent mechanisms, J. Cell. Physiol. 227 (2012) 2578–2585.
[69] J.-S. Kim, B.A. Diebold, B.M. Babior, U.G. Knaus, G.M. Bokoch, Regulation of Nox1 activity via protein kinase A-mediated phosphorylation of NoxA1 and 14-3-3 binding, J. Biol. Chem. 282 (2007) 34787–34800.
[70] S.R. Lee, et al., Reversible inactivation of the tumor suppressor PTEN by H2O2, J. Biol. Chem. 277 (2002) 20336–20342.
[71] J. Cao, et al., MC1R is a potent regulator of PTEN after UV exposure in melanocytes, Mol Cell 51 (2013) 409–422.
[72] R. Buscà, C. Bertolotto, J.P. Ortonne, R. Ballotti, Inhibition of the phosphatidylinositol 3-kinase/p70(S6)-kinase pathway induces B16 melanoma cell differentiation, J. Biol. Chem. 271 (1996) 31824–31830.
[73] M. Khaled, Glycogen synthase kinase 3beta is activated by cAMP and plays an active role in the regulation of melanogenesis, J. Biol. Chem. 277 (2002) 33690–33697.
[74] M. Khaled, et al., Microphthalmia associated transcription factor is a target of the phosphatidylinositol-3-kinase pathway, J. Invest. Dermatol. 121 (2003) 831–836.
[75] B.K. Armstrong, A. Kricker, How much melanoma is caused by sun exposure? Melanoma Res. 3 (1993) 395–401.
[76] K. Jagirdar, et al., The NR4A2 nuclear receptor is recruited to novel nuclear foci in response to UV irradiation and participates in nucleotide excision repair, PLoS One 8 (2013) e78075.
[77] P.M. Pollock, et al., High frequency of BRAF mutations in nevi, Nat. Genet. 33 (2003) 19–20.
[78] L.C.W. Vredeveld, et al., Abrogation of BRAFV600E-induced senescence by PI3K pathway activation contributes to melanomagenesis, Genes Dev. 26 (2012) 1055–1069.
[79] S.J. Robinson, E. Healy, Human melanocortin 1 receptor (MC1R) gene variants alter melanoma cell growth and adhesion to extracellular matrix, Oncogene 52 (21) (2002) 8037–8046, 2002 21.
[80] C. Haddadeen, C. Lai, S.Y. Cho, E. Healy, Variants of the melanocortin-1 receptor: do they matter clinically? Exp. Dermatol. 24 (2015) 5–9.